ELSEVIER

Journal of Hydrology 208 (1998) 62–81

Journal of Hydrology

Multifractal analysis of daily river flows including extremes for basins of five to two million square kilometres, one day to 75 years

G. Pandey[a,*1], S. Lovejoy[b], D. Schertzer[c]

[a]*Department of Civil Engineering and Applied Mechanics, McGill University, Montreal, Canada*
[b]*Department of Physics, McGill University, 3600 University Street, Montreal, Quebec, Canada*
[c]*Laboratoire de Modelisation en Mechanique, BP 162 Jussieu, Paris 75005, France*

Received 11 March 1997; revised 30 March 1998; accepted 1 April 1998

Abstract

Multifractal analysis of the daily river flow data from 19 river basins of watershed areas ranging from 5 to 1.8×10^6 km^2 from the continental USA was performed. This showed that the daily river flow series were multifractal over a range of scales spanning at least 2^3 to 2^{16} days. Although no outer limit to the scaling was found (and for one series this was as long as 74 years duration) for most of the rivers, there is a break in the scaling regime at a period of about one week which is comparable to the atmosphere's synoptic maximum, the typical lifetime of planetary-scale atmospheric structures. For scales longer than 8 days, the universal multifractal parameters characterizing the infinite hierarchy of scaling exponents were estimated. The parameter values were found to be close to those of (small basin) French rivers studied by Tessier et al. (1996). The multifractal parameters showed no systematic basin-to-basin variability; our results are compatible with random variations. The three basic universal multifractal parameters are not only robust over wide ranges of time scales, but also over wide ranges in basin size, presumably reflecting the space–time multiscaling of both the rainfall and runoff processes.

Multifractal processes are generically characterized by first-order multifractal phase transitions: qualitatively different behavior is shown for the extreme events in which the probability distributions display algebraic fall-offs associated with (nonclassical) self-organized critical (SOC) behavior. Using the observed flow series, the corresponding critical exponents were estimated. These were used to determine maximum flow volume exponents and hence to theoretically predict maximum flow volumes over aggregation periods ranging from 2^3 to 2^{16} days. These theoretical predictions are based on four empirical parameters which are valid over the entire range of aggregation periods and compare favourably with the standard (GEV) method for predicting the extremes, even though the latter implicitly involve many more parameters: three different exponents for each aggregation period. While the standard approach is essentially ad hoc and assumes independent random events and exponential probability tails (which, we show, systematically underestimate the extremes), the multifractal approach is based on the clear physical principle of scale invariance which (implicitly) involves long-range dependencies, and which (typically) involves nonclassical algebraic probabilities.

Keywords: Multifractal analysis; Daily river flows; Extremes

1. Introduction

River runoff is a major component of the hydrological cycle. It occurs over a wide range of space–time scales, from individual channel links to basins of

* Corresponding author.
[1] Now at Climate Research Division, Scripps Institution of Oceanography, University of California, San Diego, 9500 Gilman Drive, La Jolla, CA 92093-0224, USA; e-mail: gpandey@ucsd.edu

0022-1694/98/$19.00
PII S0022-1694(98)00148-6

continental size and from a fraction of a second to geological time scales. However, there exist several similarities between small and large scale river runoff characteristics. For example, Hurst (1951) reported that the runoff from various rivers exhibits long-range statistical dependences, indicating that water storage and runoff processes occur over a wide range with no characteristic time scale. Similarly, works by Benson (1962); Benson (1964), Strahler (1964), Thomas and Benson (1970) and many others have shown that the runoff characteristics, such as statistical moments and flood quantiles, are power-law functions of the corresponding basin area. Thus the river runoff over various ranges of scales is scaling (follows a power law) in space and time.

In spite of this, and although river runoff analysis and modelling has been a central concern in hydrological science for the past three decades, scaling has received very little attention. The dominant approaches have been various autoregressive multivariate models, such as AR, ARMA etc. (see, e.g., Salas, 1993). Such nonscaling models are not only incompatible with the observed scaling behavior of river runoff, such as Hurst (1951), but they have other unsatisfactory properties such as the generation of negative flows. Until very recently, the only exceptions were the mono scaling approaches for modelling the observed runoff time series (Mandelbrot and Wallis, 1968; Mandelbrot and Wallis, 1969) — essentially generalizations of Brownian motion).

In order to statistically characterize the observed flood peaks, a large number of ad hoc distribution functions and an equally large number of parameter estimation techniques have been proposed (Cunnane, 1988; Haktanir, 1992). In spite of their abundance and increasing mathematical sophistication, the selection of one rather than another is not based on physical principles. There is no a priori reason why any one of these would be compatible with the actual regional flood generating process (Potter and Lettenmaier, 1990). As pointed out by Hubert et al. (1993), in the absence of any connection with physical processes, the role of the hydrologist is reduced to fitting essentially arbitrary probability distribution functions to the observed data using ad hoc statistical goodness-of-fit criteria. Thus, there is a wide gap between mainstream mathematical modelling and our physical understanding of streamflow processes (see, e.g., Dooge, 1986; Pilgrim, 1986; Klemes, 1986).

During the last 15 years great progress has been made in studying scaling processes. In particular, it is now known that, while fractals are adequate for dealing with scaling geometric sets, multifractals are the appropriate framework for scaling fields and time series. Multifractals thus provide the natural framework for analyzing and modelling various geophysical processes that are scaling over a range of space and time scales. More specifically, for rain and clouds, first mono fractal fields (Lovejoy, 1981; Lovejoy, 1982; Lovejoy and Mandelbrot, 1985; Lovejoy and Schertzer, 1986) and then multifractals have been used to study the scaling behavior of many geophysical fields, including those of direct relevance to streamflow such as radar rain reflectivities (Schertzer and Lovejoy, 1985; Lovejoy et al., 1987; Lovejoy and Schertzer, 1990a; Gupta and Waymire, 1993; Lovejoy et al., 1996), lidar rain reflectivities (Lovejoy and Schertzer, 1990b), rain gauge series (Duncan, 1993; Fraederich and Larnder, 1993; Tessier et al., 1993; Olsson et al., 1995a; Olsson et al., 1995b), river networks (Ijjasz-Vasquez et al., 1992; Rinaldo et al., 1992; Rodriguez-Iturbe et al., 1992), clouds (Schertzer and Lovejoy, 1987a, b; Gabriel et al., 1988; Lovejoy and Schertzer, 1990a; Lovejoy et al., 1993; Tessier et al., 1993; Davis et al., 1994), extreme rainfall accumulations (Hubert et al., 1993), and topography (Lavallee et al., 1993; Lovejoy et al., 1995). In addition, the rainfall process — which is the principal input for streamflow generation — respects a scale invariance symmetry which can be exploited to model it over a range of scales by multiplicative cascade models (see, e.g., Lovejoy and Schertzer (1995) for a review) which yield multifractal space–time fields (Marsan et al., 1996; Over and Gupta, 1996). Finally, Liu and Molz (1997) have shown that hydraulic conductivities of rocks in boreholes are multifractal, and Lovejoy et al. (1998) have studied the corresponding diffusive transport.

In particular, multifractals naturally contain singularities of extreme orders and generically exhibit algebraic decays of the extreme events (associated with self-organized criticality); they can provide a sound theoretical framework to describe the observed extremes in the river runoff series. An important

generic property of multifractals is that their extremes are power-law functions of their space–time resolutions and can therefore be readily used to disaggregate the properties of river runoff time series from coarser (say, monthly series) to finer (say, weekly or daily) time scales. Hubert et al. (1993) have shown that multifractals can be used to characterize the observed accumulated maximum rainfall volume over a wide range of scales. Thus it is logical to examine the applicability of multifractals to modelling of river flow series and flood peaks over a range of space and time scales. Recently, Gupta et al. (1994) reported that streamflows are multiscaling with basin area, whereas Turcotte and Greene (1993) reported the algebraic decay of the probability distribution of annual peaks from several rivers. More recently, Tessier et al. (1996) — using 30 small basin rivers in France — carried out the first multifractal analysis of river flow data. Their analysis from one day to 30 years not only showed that river runoffs are multifractal, with two regions separated at the 'synoptic maximum' (roughly two weeks), but also provided a much broader framework to model the rainfall–runoff processes, starting from variables such as topography, river network, etc. that generate and modify the streamflow through the basin. In this paper we obtain quantitatively similar results on basins with a much wider range of scales; this shows that our characterization is robust. In addition to their use for studying phenomena over wide ranges of time and space scales, multifractals provide a natural framework for studying them over the full range of intensities up to the most extreme.

The main objective of this paper is to study the behavior of the streamflow series over a range of space and time scales using the multifractal framework; in particular we extend the Tessier et al. (1996) results both to larger basin sizes and to a detailed study of the extremes. The paper is organized as follows. First we give a brief description of the river flow data used in the study (Section 2). A spectral analysis of the river flow data is given in Section 3. This is followed by a discussion of universal multifractals (Section 4) and the extremes with their relation to SOC (Section 5). The characterization of maximum volume as a function of interval duration under a multifractal framework has been provided in Section 6.

2. Data

The flow data we analyzed are the daily streamflow data from 19 gauging stations from the continental USA. Those stations were selected randomly from the USGS gauging station list and represent basins of very different characteristics. Table 1 presents the summary of the stations used in the study. The areas of the basin range from 5 to 1.8×10^6 km^2, covering nearly six orders of magnitude. The lengths of the series vary from 3422 to 26 663 days. The observed flow series were normalized by dividing by the at-site mean. The objective of the normalization was to take out the basin size effect from the observed flow series, which come from basins of various sizes, to allow quantitative statistical comparison of different rivers (for example, to obtain meaningful 'ensemble' statistics, used below). The total overall size of the ensemble normalized flow data set was an equivalent of 670.04 station years. Specific differences with the data used in the Tessier et al. (1996) study include the much wider range of scales of basins (the latter were in the range of 40–200 km^2) and the fact that the latter had very little human intervention.

3. Spectral analysis and scaling regimes

The power spectrum of any field or series (daily river flow data, in the present case) is by definition an ensemble average quantity; a fact that must be borne in mind when it is estimated from only one or a few series. If each series is regarded as a different realization of a multifractal process, then we expect significant random series-to-series variability because multifractal processes are highly intermittent (i.e., their sample-to-sample variability is much larger than that expected by classical statistics). This intermittency can be so extreme that certain structures or fluctuations are almost surely absent in individual realizations while simultaneously being almost surely present on a large enough ensemble of realizations. In other words, they are not ergodic (see Schertzer and Lovejoy (1989) and Section 5 below for the notion of 'sampling dimension' which can be used to quantify this). If the spectra from different basins are not very different from each other, then the various series may belong to the same ensemble. However, the power

Table 1
Description of the stations used in the study, in order of increasing basin size

Station name	Basin area (km^2)	Data records (days)	Mean flow ($m^3 s^{-1}$)
Rocky Brook, MA	5	7670	0.1
Pendleton Hill River, CT	10	12784	0.2
Kettle Brook, MA	82	20137	1.3
Mill River, MA	86	4674	1.2
North Nashua River, MA	164	7670	3.5
Yantic River, CT	231	20819	4.7
Indian Creek, CA	311	3422	11.6
Mccloud River, CA	927	22829	25.7
Ohoopee River, GA	2875	20583	28.7
Grand River, MO	5827	26663	34.8
Sabine River, TX	16856	10135	28.7
Osage River, MO	37555	22676	300.1
Pecos River, NM	50608	20454	4.5
Canadian River, OK	67182	5022	18.6
Susquehanna River, PA	67314	22646	1042.3
Rio Grande River, NM	79772	22448	19.2
Arkansas River, OK	250385	16434	552.7
Colorado River, CO	638950	16709	135.2
Mississippi River, MO	1805222	21733	5150.8
Total no. of days for the ensemble: 244566 = 670.04 Station years			

spectrum is a sensitive indicator of the range of scales over which a field is scaling. For any scaling field, the power spectrum has a power-law dependency on the corresponding frequency; that is:

$$E(\omega) \approx \omega^{-\beta} \quad (1)$$

in which ω is the frequency, β is the spectral exponent, and $E(\omega)$ is the energy of the spectrum. Eq. (1) states that for any scaling field there exists a log–log linear relation between the frequency and the corresponding power spectrum.

Spectral analysis was conducted on all individual series as well as being averaged over the ensemble of normalized flow series (note that, due to the variable length of the series, the number of series contributing to the low frequency part of the spectrum depends somewhat on frequency; see below). The power spectra from the smallest, largest and some other basins having intermediate areas are shown in Fig. 1a, and the ensemble of normalized flow series is shown in Fig. 1b. The log–log linearity shows that daily river flow series have two scaling regimes with a break separating them at about one week. The average β for individual flow series on the low frequency side ($\sim$ one week to 10 years) was found to be 1.17 ± 0.34, where the standard deviation represents the series-to-series variation of β about the mean; for the ensemble normalized flow series the corresponding low frequency value was 0.72 ± 0.30 whereas, for the high frequency regime (one day to one week), $\beta \approx 2.47$, corresponding to much smoother variations. Although no clear outer limit to the scaling was found (for some rivers this was more than 73 years), for most of the rivers there is a break in the scaling at high frequencies; note that the extreme two lowest frequencies have little statistical weight since they correspond only to one or a few rivers and one or two long fluctuations.

The time scale of the break varied between 3 and 24 days with an average value of less than 6 days (obtained using the ensemble spectrum). For some rivers there are dominant cycles at some specific time intervals, typically at 3, 4 and 7 days, which are known to be the results of the alteration of the river regimes by human intervention involving artificial regulating structures such as dams and barrages (see, e.g., e, h in Fig. 1a). Many of these structures are operated following strict schedules such as sediment flushing, release of water for consumptive uses, periodic inspections of the parts and

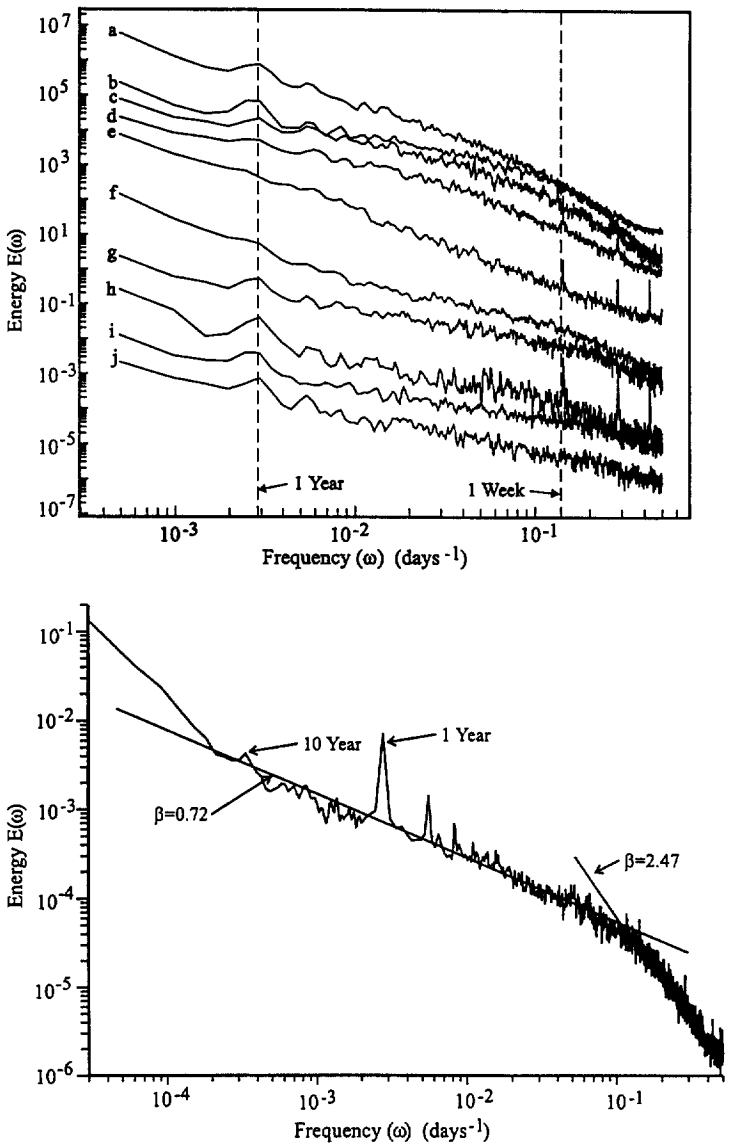

Fig. 1. *a*, Energy spectra of daily river flow series from different river basins from the continental USA: (a) Mississippi River, (b) Susquehanna River, (c) Arkansas River, (d) Osage River, (e) Colorado River, (f) McCloud River, (g) North Nashua, (h) Mill River, (i) Pendleton Hill, (j) Rocky Brook (in order of decreasing mean flow rate). *b*, Power spectra for the normalized flow series from 19 river basins. The series were obtained by diving the observed flow series by respective means and combining together the resulting series from all sites.

machineries, etc.; these periods resulted in sharp spectral peaks in several of the series. In addition to artificially induced periodicities, the spectra also show that river flow series have annual cycles. The dominant annual cycle of the river flow series can be seen from the power spectra of the ensemble spectrum (Fig. 1b). In view of the break in the scaling regimes at about one week, in the following analysis the smallest scale of aggregation will be taken as 8 days. These findings are similar to those reported earlier by Tessier et al. (1996) using the hydrologic data from 30 river basins from France having areas between 40 and

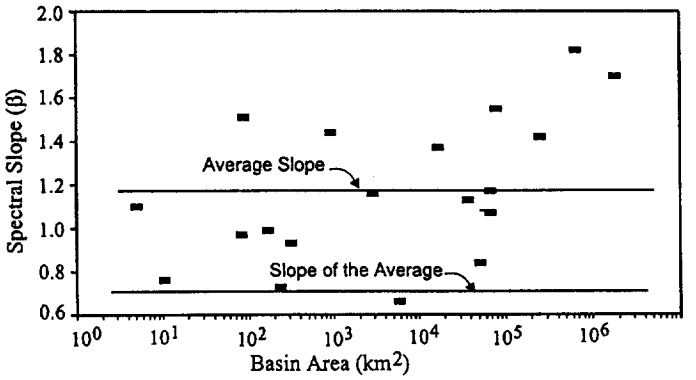

Fig. 2. Variation of the spectral slope with the basin area. The average slope corresponds to the average of all fitted individual slopes whereas the slope of the average is the slope of the power spectrum for the ensemble of normalized flow series.

200 km^2. They include the values of β; see Table 3 for a comparison. However, in Tessier et al. (1996) the time of the break varied between 10 and 30 days with an average value of 14 days. This difference may be due to the increased effective storage (see below). A scatter plot between the scaling exponent (β) as a function of basin size (A) is indicated in Fig. 2. There is no clear systematic pattern in the basin-to-basin variability of the spectral slopes; the differences can probably be attributed to the statistical sample-to-sample variability. Recall that on a single realization β is simply a statistical estimate of the ensemble value; in multifractals it can be quite variable from one realization to another.

River runoff phenomena are the combined effects of the precipitation process (either rainfall or snow melt) and the response of local watershed characteristics such as antecedent conditions of the soil moisture, pore size, channel geometry, local geology, sediment type, climatic and other factors to the precipitation input. Thus, the gauged river runoff reflects the overall behavior of the complex interactions which prevailed between precipitation input and the basin factors that modify it. It seems likely that the rainfall process possesses a scale invariance symmetry over a range of scales and there is a break in the scaling regime for a time period of about two weeks. This time is roughly the 'synoptic maximum' characteristic of meteorological fields including the rainfall process (see Koloshnikova and Monin (1965) for the pressure field; Lovejoy and Schertzer (1986) for the temperature field; and Tessier et al. (1993); Tessier et al. (1996) for discussions on rain). The synoptic maximum is the typical lifetime of structures of planetary extent and provides a natural scale for separating meteorological from climatological regimes. In the case of river runoff, the maximum scale is the basin area and during the transition (that is, when the precipitation becomes river runoff) it is expected that those basin factors will smooth out the precipitation break associated with the synoptic maximum scale of the input (see Gupta and Waymire (1997) for the runoff-generation mechanisms on hillsides and for the time-scale separation of surface and subsurface flow velocities). The decrease in the break in scaling regimes (from about 16 days for the small basins studied by Tessier et al. (1996) to about 6 days here) is presumably due to this increased smoothing effect; however, further study is warranted in this regard.

4. Multifractals

4.1. Properties

The basic equation for the scaling of the probability distributions of multifractal fields is (Schertzer and Lovejoy, 1987a, b)

$$Pr(R_\lambda > \lambda^\gamma) \approx \lambda^{-c(\gamma)} \tag{2}$$

where $\lambda = T/\tau$ is the scale ratio, R_λ is the intensity of field at scale λ, γ is the order of singularity, T is the longest duration of interest and τ is the duration of observation. Eq. (2) states how the probability distributions of singularities of order γ vary as a

function of scale; the scale-invariant exponent is the codimension function $c(\gamma)$; the $\approx$ sign indicates equality to within factors slowly varying with respect to λ. The scaling of probabilities also implies the scaling of the qth order statistical moments, given by

$$<\phi_\lambda^q> = \lambda^{K(q)}, \quad \lambda > 1 \tag{3}$$

where $K(q)$ is the multiple scaling exponent function for the moments. The exponents $K(q)$ and $c(\gamma)$ are related to each other via the Legendre transform (Parisi and Frisch, 1985) as

$$c(\gamma) = \max_q (q\gamma - K(q)) \tag{4}$$

$$K(q) = \max_\gamma (q\gamma - c(\gamma))$$

A priori, the only restriction on $c(\gamma)$ and $K(q)$ is that they must be convex. Although the nonlinear cascade dynamics relating one scale to another scale are complex, Schertzer and Lovejoy (1987b) have argued that cascade processes possess stable (attractive) universal generators and hence are insensitive to the details of dynamics (see also Schertzer et al. (1995) on the debate about strong versus weak universality and Schertzer and Lovejoy (1997) for more debate about universality, especially in rain; for other references on multifractals with Levy generators, see Brax and Peschanski, 1991; Evertsz and Mandelbrot, 1992; Gupta and Waymire, 1993). The universal $K(q)$ functions for a conservative process (i.e., the direct result of a multiplicative cascade, see below) are given as

$$K(q) = \begin{cases} \dfrac{C_1(q^\alpha - q)}{\alpha - 1} & \text{for } \alpha \neq 1 \\ C_1 q \log(q) & \text{for } \alpha = 1 \end{cases} \tag{5}$$

$$c(\gamma) = C_1 \left(\frac{\gamma}{C_1 \alpha'} + \frac{1}{\alpha} \right)^{\alpha'} \quad \text{for } \alpha \neq 1 \tag{6}$$

in which $0 \leq \alpha \leq 2$ is the multifractal index, $0 \leq C_1 \leq D$ is the codimension of the mean of the field and $1/\alpha + 1/\alpha' < 1$, D is the dimension of the observing space ($D = 1$ for time series). The value of the multifractal index (α) is also the order of the generator's levy distribution and it quantifies the distance of the process from monofractality. When $\alpha = 0$, the process is monofractal, whereas $\alpha = 2$ corresponds to 'lognormal' multifractals, due to the divergence of moments this is somewhat a misnomer. For nonconservative processes a third parameter H (described later) is needed. Universal multifractals are the multiplicative cascade analogues of Levy processes which are stable, attractive processes for addition of random variables (Brownian motion being a special case); they are thus believed to be the generic consequences of scaling nonlinear dynamics with a large number of degrees of freedom. A basic realistic property of multifractal models is that they are able to simulate the intermittency and extreme variability present in the field while preserving the statistical properties over a wide range of scales.

4.2. Estimation of the universal multifractal parameters

For the observed daily flow series, the parameters α and C_1 of the multifractal model were estimated using the double trace moment (DTM) technique (Lavallee et al., 1993). The q, η double trace moment at resolution λ and Λ is defined as

$$Tr_\lambda (\phi_\Lambda^\eta)^q = \left\langle \sum_i \left(\int_{B_{\lambda,i}} \phi_\Lambda^\eta d^D x \right)^q \right\rangle \propto \lambda^{K(q,\,\eta)-(q-1)D} \tag{7}$$

where the sum is over all the disjoint D dimensional balls $B_{\lambda,i}$ (here intervals of length $\tau = T/\lambda$) required to cover the time series, and $K(q, \eta)$ is the double trace scaling exponent and $K(q, 1) = K(q)$ is the scaling exponent. A simpler way of expressing this is

$$\langle (\phi_\Lambda^\eta)_\lambda^q \rangle = \lambda^{K(q,\,\eta)} \tag{8}$$

where the notation indicates that the multifractal ϕ at a (finest) resolution Λ is first raised to the power η, degraded to resolution λ, and the qth power of the result averaged over the available data. The scaling exponent $K(q, \eta)$, related to $K(q, 1) \equiv K(q)$, is given by

$$K(q,\,\eta) = K(q\eta,\,1) - qK(\eta,\,1) \tag{9}$$

Thus, in the case of universal multifractals, plugging Eq. (5) into Eq. (9), $K(q, \eta)$ has a particularly simple

dependence on η:

$$K(q, \eta) = \eta^{\alpha} K(q) \tag{10}$$

α can therefore be estimated on a simple plot of $K(q, \eta)$ vs $\log(\eta)$ for fixed q.

The DTM technique yields direct estimates of the parameters from conservative multifractal fields (the direct results of a multiplicative cascade process; the conservative quantity is a flux which is conserved while going from one scale to other). However, a priori, there is no reason to expect that an observed quantity such as river flow should be a conserved field. Rather, following the fractionally integrated flux (FIF) model (Schertzer and Lovejoy, 1987b; Schertzer et al., 1997), it will be connected to the underlying conserved field via fractional integration/differentiation of various orders (see Oldham and Spanier (1974), Ross (1975) for the latter). The order of the integration/differentiation required is H, which since the latter are low convolutions, is a basic long-range dependency factor, written H in honour of Hurst. Theoretically, since H is the degree of fractional integration needed to obtain the observed runoff series from the underlying conserved series, we should differentiate by order H (e.g., by power-law Fourier filtering) to invert the scale-invariant process and recover the conserved field. However, Lavallee et al. (1993) have shown that it is sufficient to differentiate by order $\geq H$. Hence, in the present study, in order to get a conserved series, the original series were replaced by their (absolute) first derivatives, approximated by the absolute first differences of the series. This is equivalent to assuming $H < 1$; an assumption which we verify a posteriori below. Since the absolute slope of the power spectrum (β) for the majority of the river series including the ensemble is close to unity (see Table 2), assuming a priori a value of $H < 1$ is fairly reasonable; indeed, we find for the low frequency regime $H \approx -0.03 \pm 0.14$, i.e., it is perhaps conserved ($H = 0$), so in this regime the differencing may not be necessary.

The double trace moments for the ensemble flow series for an aggregation period of 8 days are shown in Fig. 3a. The log–log linearity between the trace moments and the scale ratio λ shows the scaling nature of the streamflow series. The corresponding plots of the scaling exponent $K(q, \eta)$ vs η are shown in Fig. 3b. The DTM estimated values of α and C_1 are given in Table 2. The average value of the parameter α from the individual series is 1.65 ± 0.12, whereas the corresponding value for the ensemble is 1.70 ± 0.11. Thus the generators (roughly the logs of the conserved quantities) of the daily river flow series are somewhere between (an asymmetrical) Cauchy ($\alpha = 1$) and the normal ($\alpha = 2$). An examination of the variability of these parameters shows that there is no systematic variation with basin area; thus the difference can be attributed to series-to-series variability rather than to the area effect (due to the large intermittency, α requires very large samples for accurate estimation). Further, Eq. (6) shows that when $\alpha > 1$, $\alpha' > 2$ and the singularities (γ) are unbounded. In this case it can be shown that we expect algebraic tails associated with the multifractal phase transition and self- organized criticality (Schertzer and Lovejoy, 1997; Schertzer and Lovejoy, 1998). From the estimated values of α and C_1, and taking the spectral slope (β) of the conserved process, the value of exponent H — the order of fractional integration required to go from the conserved to the nonconserved (observed) process — is given by (Lavallee et al., 1993)

$$H = \frac{\beta - 1 + K(2)}{2} \tag{11}$$

in which $K(2)$ can be estimated from C_1 and α using Eq. (5). The average value of H from individual series is 0.20 ± 0.15 whereas for the normalized flow series it is -0.03 ± 0.14. The variability of the exponent H with the basin area, as shown in Table 2, also supports the hypothesis that the series-to-series variability is the result of random sample-to-sample variability.

The results reported by Tessier et al. (1996) are compared with the present findings in Table 3. In comparison, Tessier et al. (1996) find $\alpha = 1.45 \pm 0.2$, $C_1 = 0.20 \pm 0.1$, $H = -0.05 \pm 0.2$ for the low frequency runoff, values which are very close to those found here (see Table 3). If the parameters α, C_1 and H are universal for all river runoff series, which is consistent with the similarity of the parameters found here and by Tessier et al. (1996), and — as argued in that paper — C_1 and α are roughly the same as for precipitation (Tessier et al. (1996) find $C_1 \approx 0.1 \pm 0.05$ and $\alpha \approx 1.6 \pm 0.2$), then the only low frequency statistical difference between precipitation and flow series is the degree of fractional integration H. In this case, the value of H can be

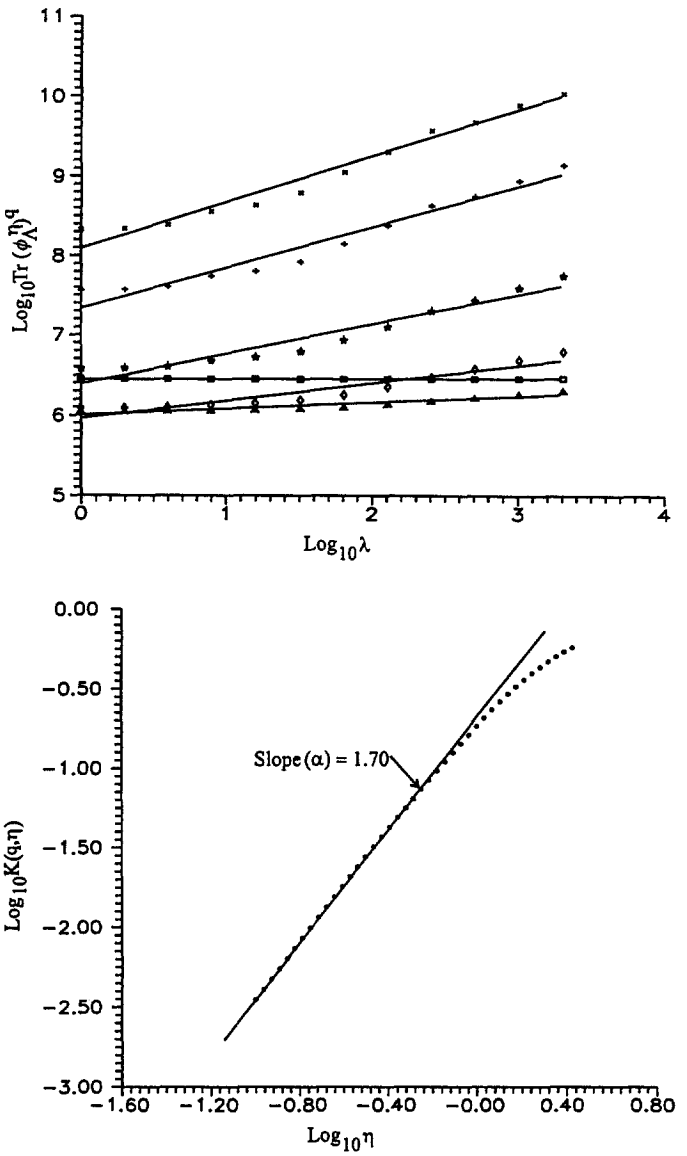

Fig. 3. *a*, Log of the trace moment vs log of λ for $q = 2$, for the ensemble of normalized flow series aggregated at 8 days to 16 384 days. From top to bottom, $\eta = 2.45, 2.08, 1.5, 0.99, 0.52$ and 0.1. *b*, Log $K(q, \eta)$ vs log η using $q = 2.0$ for normalized flow ensemble aggregated at 8 days interval.

used to determine a linear transfer function relating the river runoff series to observed rainfall series. For example, taking a value of $H \approx -0.35$ for low frequency rainfall series, as reported by Tessier et al. (1996), and in order to get the river runoff time series to have the same statistics as that of the rainfall time series, fractional integration of order $H \approx -0.03 - (-0.35) \approx 0.32$ is required. Note that if α and C_1 are different for rain and river flow, then nonlinear transformations are necessary.

5. The distribution of extremes

5.1. Power law distribution and self-organized criticality

For multifractal processes the variability of the field goes down to such small scales that the typical measurements are at much larger scales; for example, the river flow is clearly variable at time scales much

Table 2

Multifractal parameters for the daily river runoff series (the error estimates are the dispersions of the corresponding parameters estimated from the individual series)

Basin area (km^2)	Parameters			
	β	α	C_1	H
5	1.1	1.38	0.13	0.15
10	0.76	1.74	0.11	− 0.02
82	0.97	1.8	0.12	0.1
86	1.51	1.69	0.07	0.32
164	0.99	1.66	0.12	0.1
231	0.73	1.7	0.11	− 0.04
311	0.93	1.69	0.19	0.13
927	1.44	1.77	0.16	0.37
2875	1.16	1.62	0.13	0.19
5827	0.66	1.46	0.18	− 0.02
16856	1.37	1.44	0.13	0.29
37555	1.13	1.71	0.13	0.18
50608	0.84	1.74	0.26	0.16
67182	1.07	1.61	0.16	0.17
67314	1.17	1.65	0.11	0.18
79772	1.55	1.51	0.08	0.34
250385	1.42	1.69	0.14	0.33
638950	1.82	1.72	0.08	0.48
1805222	1.7	1.69	0.07	0.41
Average	1.17 ± 0.33	1.65 ± 0.12	0.13 ± 0.05	0.20 ± 0.15
Ensemble of normalized flows	0.72 ± 0.30	1.70 ± 0.11	0.12 ± 0.03	− 0.03 ± 0.14

less than a day. The measurements therefore average out much of the corresponding small-scale variability. However — contrary to the usual assumptions — not all of the small-scale variability is smoothed out in this way. In particular, for multifractal processes, we expect that the statistics of the averaged quantities will generally be quite different from those of the corresponding field whose dynamics have been stopped at the observation scale. The latter are the (theoretical) 'bare' quantities whereas the empirically measured ones (averages over small-scale activity) are the 'dressed' quantities. While the bare quantities follow Eq. (3) with $K(q)$ finite for all q, the dressed quantities follow Eq. (3) up to a critical moment q_D after which they diverge; that is:

$$< \phi_\lambda^q > \rightarrow \infty \text{ for } q \geq q_D \tag{12}$$

The divergence of the statistical moments corresponds to the hyperbolic fall-off of the probability distribution; that is:

$$Pr(\phi_\lambda \geq s) \approx s^{-q_D} \text{ for } s \gg 1 \tag{13}$$

in which s($\gg$ 1) is a threshold and ϕ_λ is the integrated field at scale λ. The divergence of high order

Table 3

Comparison of estimates of parameters β, α, C_1 and H for the ensemble of 30 river and rainfall series (small basins, Tessier et al. (1996), from one month to 11 years, ratio 2^{10}) and the ensemble of 19 (normalized) river series 8 days to 11 years, ratio 2^{12}; this study). Comparing the last two lines, we see that the means of all the parameters fall within the corresponding one standard deviation error bars, indicating that the small and large basin parameters may well be the same

Reference	Parameters					
	β	α	C_1	H	q_S	q_D
Tessier et 'al. (1996) (rain)	0.2 ± 0.1	1.6 ± 0.2	0.10 ± 0.05	− 0.35 ± 0.2	5.2 ± 0.5	3.6 ± 0.7
Tessier et al. (1996) (flows)	0.5 ± 0.1	1.45 ± 0.2	0.20 ± 0.1	− 0.05 ± 0.2	4.2 ± 0.5	3.2 ± 0.7
This paper (flows)	0.72 ± 0.3	1.70 ± 0.11	0.12 ± 0.03	− 0.03 ± 0.14	3.5 ± 0.6	3.1 ± 0.7

statistical moments (Eq. (12)) and the equivalently power-law distribution of the extremes (Eq. (13)) are the direct consequences of the multifractality. The dressed codimension function $c_d(\gamma)$ relevant to the hyperbolic region can be defined:

$$c_d(\gamma)=\begin{cases} c(\gamma) & \text{for } \gamma \le \gamma_d = K'(q_D) \\ c(\gamma_D)+q_D(\gamma-\gamma_D) & \text{for } \gamma > \gamma_d \end{cases} \tag{14}$$

This associated quantitative change of behavior at γ_D (equivalently, q_D) can be theorized as a multifractal phase transition (Schertzer et al., 1993; Schertzer and Lovejoy, 1998) yielding self-organised critical (SOC) events (Bak et al., 1987; Bak et al., 1988; Bak et al., 1990).

In general, the upper limit of the exponent q to which the statistical moments will remain finite (i.e. q_D) depends upon the type of field and the dimension (D) over which it is integrated or averaged (hence the subscript). However, in general any finite number of samples will almost surely miss the presence of rare extremes in the field and hence empirical singularities will have a maximum singularity γ_s. If we have N_s independent samples, each with a range of scales λ, larger and larger portions of the probability space will be explored and more extreme singularities will be encountered. Hence, the sampling dimension D_s can be introduced to account for the fraction of the probability space actually explored (Schertzer and Lovejoy, 1989):

$$D_s=\frac{\log N_s}{\log \lambda} \tag{15}$$

i.e., only singularities $\gamma < \gamma_s$ with $c(\gamma_s) = D + D_s$ can be observed. Note that this equation (and hence Eq. 16 below) has only recently been given vigorous mathematical proof, and this only in the special case $\alpha = 2$, $D = 1$, $D'_s = 0$! (G.M. Molchem, private communication). In other words, the process is generally nonergodic and D_s quantifies this. The total dimension of the explored space thus becomes $D + D_s$, where D is the dimension of the embedded space, $D = 1$ for time series. Since there is a one-to-one correspondence between the order of singularity and the moments (Eq. (4)), there will be a maximum order of moment which can be accurately estimated: $q_s = c(\gamma_s)$. For (bare) universal multifractals, this is

$$q_s=\left(\frac{D+D_s}{C_1}\right)^{1/\alpha} \tag{16}$$

Thus, for small samples with $q_s < q_D$, the divergence of moments is not observable. For $q \ge q_s$ the moment estimates will be dominated by the largest (most extreme) events in the sample, which leads to the linear rather than convex $K(q)$ (corresponding to a second-order multifractal phase transition).

Now consider $q_s > q_D$, or equivalently $\gamma_s = K'(q_s) > \gamma_D = K'(q_D)$. In this case we must use the dressed codimension so that $c_d(\gamma_{sd}) = D + D_s$. This is shown systematically in Fig. 6. For $q_s > q_D$ we then obtain a more violent first-order multifractal phase transition at $q = q_D$: a discontinuity in the first derivative of $K(q)$.

The probability of exceedances as a function of the threshold discharge for some typical river basins is shown in Fig. 4a. Similar plots were obtained for the other river basins as well. For the ensemble of normalized flows, the plot of the threshold discharge against the probability of exceedance is given in Fig. 4b. The plot plausibly shows the algebraic nature of the decay of the distribution of the extreme flows. The flattening of the distribution for small discharges is due to the fact that the power law behavior takes place only after a certain threshold ($\gamma > \gamma_D = K'(q_D)$), as given by Eq. (12) and (13). The deviations in the very large values of discharges may be the results of the finite sample size at this range. Using the multifractal parameters, the theoretical values of the exponents (q_s) were also determined and are shown in Table 4. The slopes of the best-fit straight lines (q_D) for the extremes were determined for all individual series and are given in Table 4. The value of the exponent q_D varied between 1.5 and 25. Since q_s is the highest order moment which is readily estimated, whenever $q_D' > q_s$ the estimate is suspect (actually, since D_s depends on the entire range of scales whereas the histogram is only at a single highest resolution, it is somewhat overly stringent). We therefore removed the two unusually large values of 11 and 25 for two rivers (where $q_D \gg q_s$); the average value of the resulting exponent (q_D) was 3.37 ± 0.86, which is close to the values reported by Tessier et al. (1996) which are 3.2 ± 1.5 for low frequencies but 2.7 ± 1 for high frequencies (see Table 3). Hence, the

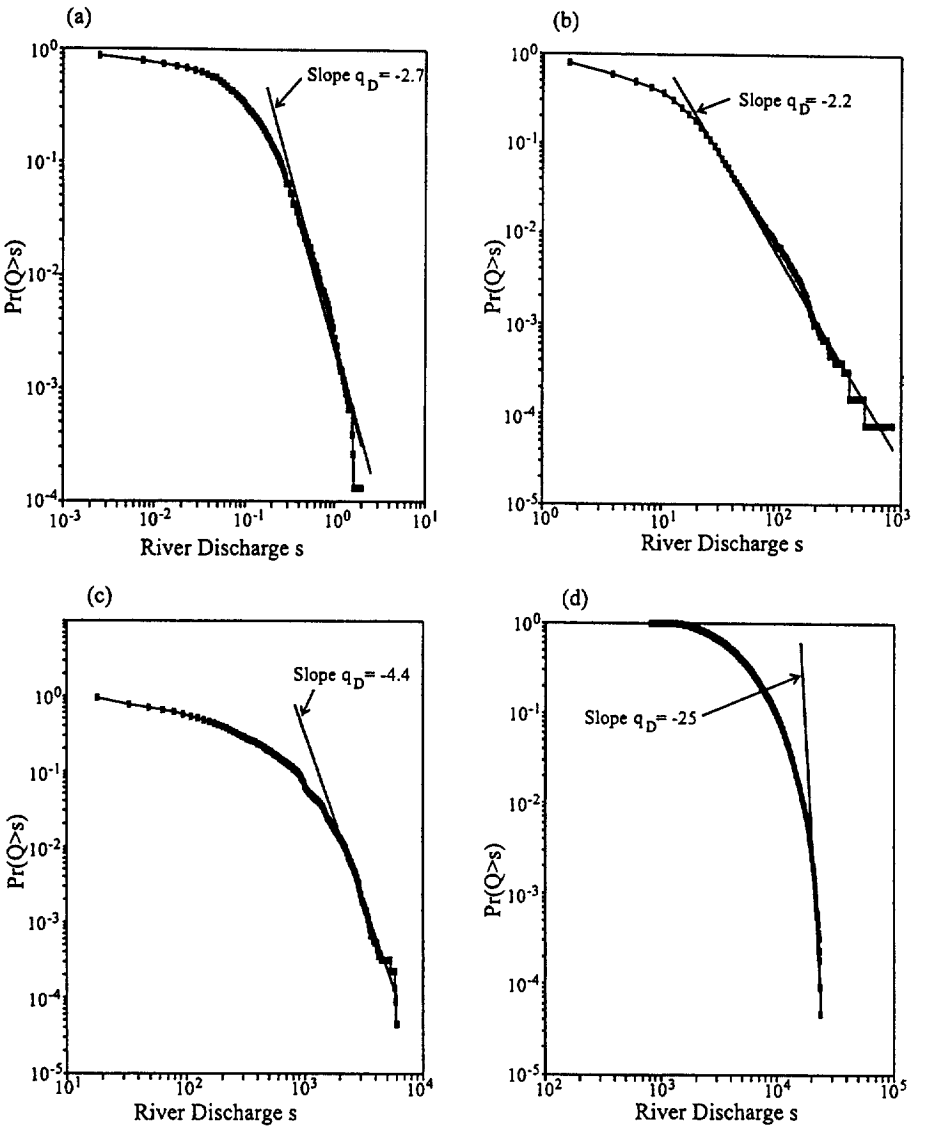

Fig. 4. *a*, Plots between the discharge (*s*) and the probability of exceedance for typical river basins: (a) Rocky Brook, (b) Indian Creek, (c) Osage River, (d) Mississippi River. The flattening of the curve at low discharge implies that the power law distribution holds only after some threshold. The fitted slopes are the estimates of the exponent q_D. *b*, Same as Fig. 3*a* but for the ensemble of normalized flows. *c*, Plots between the observed discharge (*s*), quantiles from the GEV distribution and the probability of exceedance for the normalized flow series. The slope of each line was estimated using the straight line portion at the extreme end.

approximate critical order of divergence of moments that can be determined using the observed daily data river flow series varies between 2 and 5. Those values are not so different from those reported by Turcotte and Greene (1993) (they denoted q_D by the symbol '*D*', which may cause it to be confused with a fractal dimension). The most reliable result is from the normalized ensemble which has a higher q_s, which is due to the increased number of samples (Fig. 4b); we find $q_s \approx 3.48 > q_D \approx 3.12$. Note however that the small difference between q_s and q_D shows how difficult such estimates are (they require large databases; preferably many rivers).

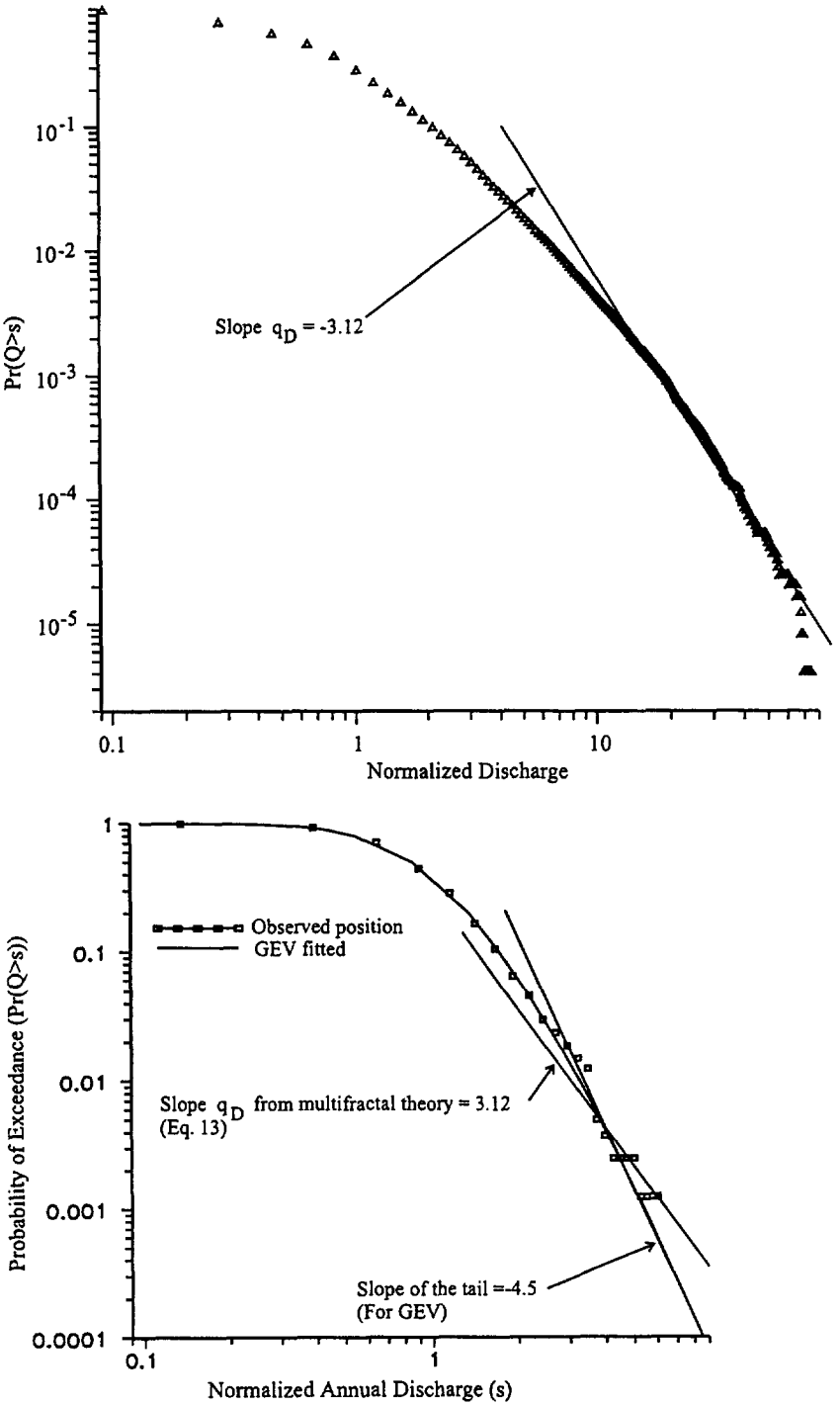

Fig. 4. (*Continued*).

Table 4

Estimation of the parameters q_s, q_D and γ_s for individual as well as normalized flow series (the average q_D was determined after excluding the last two values which had $q_D \gg q_s$ and so were judged unreliable). The singularities γ_s and $\gamma_s - H$ respectively correspond to the theoretical value (estimated using $c(\gamma_s) = D + D_s$ when $q_D > q_s$ and $c(\gamma_{sd}) = D + D_s$ when $q_D < q_s$) without and with adjustments for the filtering process, and γ_{max} is the slope of the observed maximum. The GEV fitted slope is the slope of the extreme tail of the generalized extreme value distribution (Eq. (17)). In the table, "average" corresponds to the average of individual exponents

Basin area (km^2)	q_s	q_D	γ_s (theory)	γ_{max} (observed)	$\gamma_s - H = \gamma_{max}$ (theory)	GEV fitted slope
5	4.4	2.74	0.52	0.39	0.36	6.95
10	3.6	2.37	0.51	0.49	0.53	2.54
82	3.3	2.41	0.52	0.49	0.42	2.4
86	4.8	4.9	0.41	0.25	0.09	9.6
164	3.6	3.3	0.52	0.4	0.42	5.1
231	3.7	2.57	0.54	0.48	0.58	2.8
311	2.7	2.24	0.64	0.55	0.58	2.5
927	2.8	3.5	0.61	0.28	0.24	2.8
2875	3.5	4.18	0.53	0.39	0.34	5.1
5827	3.2	3.26	0.60	0.54	0.62	6.0
16856	4.1	3.6	0.50	0.36	0.21	2.76
37555	3.3	4.42	0.55	0.39	0.37	5.44
50608	2.17	2.24	0.73	0.58	0.57	1.42
67182	3.1	4.6	0.58	0.33	0.41	44
67314	3.8	3.25	0.50	0.45	0.32	3.7
79772	5.3	4.17	0.41	0.28	0.07	2.8
250385	3.2	3.6	0.56	0.47	0.23	3.7
638950	4.3	11.3	0.44	0.16	− 0.04	2.9
1805222	4.8	25	0.41	0.19	− 0.01	10.0
Average	3.67 ± 0.8	3.37 ± 0.86	0.64 ± 0.08	0.39 ± 0.12	0.33 ± 0.2	4.9 ± 9.1
Ensemble	3.48 ± 0.6	3.12 ± 0.7	0.53 ± 0.07	0.53 ± 0.11	0.67 ± 0.17	4.5

5.2. *The standard approach*

At this point it will be useful to discuss the common engineering practice of fitting ad hoc probability distributions to the observed flood peaks. Statistical characterization of the flood series and subsequent estimation of the flood quantiles associated with a particular risk has become a subject of constant research in the hydrological sciences. The usual approach is to pick an annual maximum from the observed daily flow series (however, in some cases n highest peaks are also considered, where n is the length of the annual flood series). Assuming that those peaks represent independent stochastic events, a probability distribution function is fitted and the quantiles associated with certain risks are determined. Over the last 30 years, many probability distribution functions and an equal number of parameter estimation techniques have been developed (see Haktanir, 1992). The inferences are based upon the statistical goodness-of-fit tests and there is no attempt to give any physical justification for the choice (Potter and Lettenmaier, 1990); indeed, the assumption of statistical independence contradicts the observed scale invariance with its associated long-range correlation structure. Hence, although the methodology provides engineers with flood quantiles for design purposes, its theoretical basis is suspect. Aside from their ad hoc nature, the models are valid only over a particular (unique) aggregation time scale; that is, the inferences are valid only for the time scale for which the model is calibrated. For example, since the models are developed using the annual flood data, the inferences are valid for the annual aggregation scale. The behavior of the process at finer resolution (say monthly or weekly) as well as coarser resolution (say biannual or decadal) is not considered and these models cannot be used at other scales. Besides, it is not very difficult to see that several of these distribution functions give a very rapid

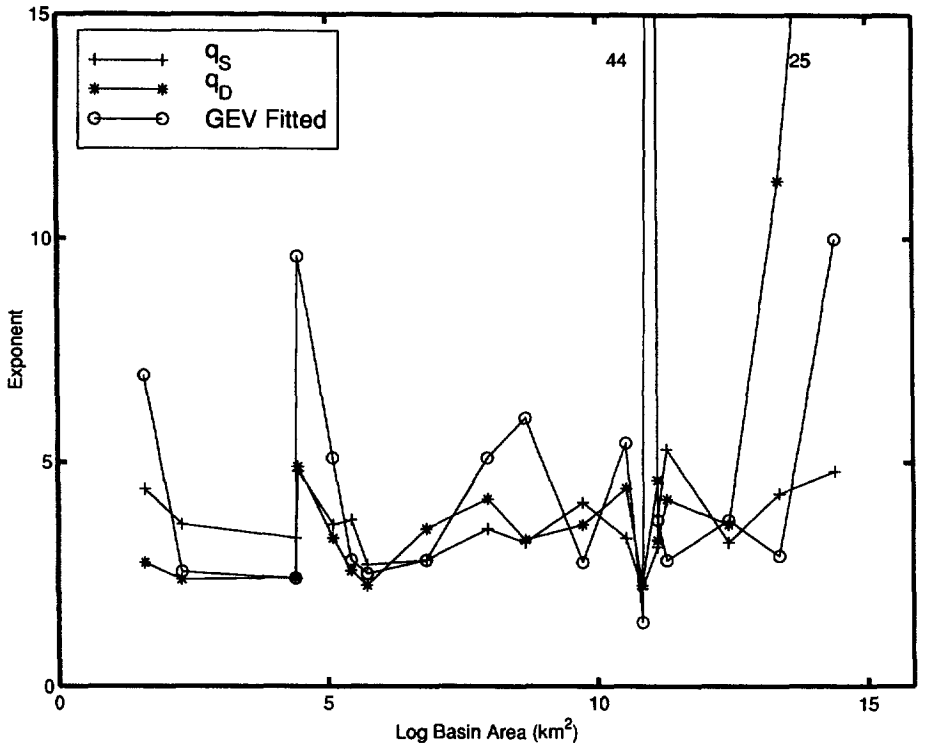

Fig. 5. Variation of the exponents q_S, q_D and q_{GEV} with basin area. The exponent q_{GEV} corresponds to the best fit of the extremes, using the GEV distribution for the annual peak flows.

fall-off ('thin', exponential) probability tail (i.e, $\log(Pr(Q > s)) \propto -s$) rather than the slow ('fat') hyperbolic (i.e., $\log(Pr(Q > s)) \propto -\log(s)$) decays of the extremes. In general, exponential distributions will not be scaling; hence they are in contradiction with the multifractal nature of the flow series (the multiscaling as a function of resolution).

Based upon intensive simulation studies, the generalized extreme value (GEV) distribution has been recommended to model the annual maximum of the observed daily flood series by the Natural Environmental Research Council (1975) (ERC), Hosking et al. (1985), Lettenmaier and Potter (1985) and Potter and Lettenmaier (1990). Due to its large number of parameters, the distribution is considered general (it notably includes the Gumbel distribution as a special case). The cumulative distribution function (cdf) or the probability of nonexceedance ($Pr(Q \leq s) = F(s)$) for the GEV distribution is given as

$$F(s) = \begin{cases} \exp\left[-(1-\{a_3(s-a_1)\}/a_2)^{1/a_3}\right], & a_3 \neq 0 \\ \exp[-\exp\{-(s-a_1)/a_2\}], & a_3 = 0 \end{cases} \quad (17)$$

where a_1, a_2 and a_3 are respectively the location, scale and shape parameters of the distribution. Note that, while at a given scale both GEV and universal multifractal distributions have three parameters (four for multifractals if we include q_D), the former requires a different empirical set of parameters for every aggregation period while the multifractal model requires only three for the entire range of aggregation scales (here $>10^3$). In addition, we will now show that even over a fixed aggregation scale the multifractal model gives a better fit to the extremes.

In order to compare and contrast this approach with the multifractal one, the GEV distribution was fitted to

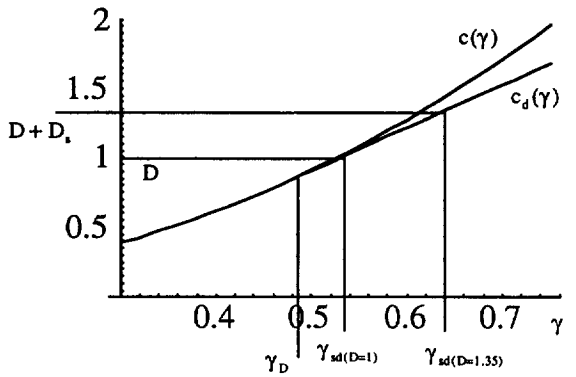

Fig. 6. Bare and dressed ($c(\gamma)$, $cd(\gamma)$) corresponding to the parameters found for the ensemble of normalized flows: $C_1 = 0.12$, $\alpha = 1.70$, $q_D = 3.12$. Also shown are various significant singularities (γ): $\gamma_D = K'(q_D)$, which is where the dressed codimension separates from the bare one. Also shown are the maximum singularities present in a single realization of dimension $D = 1$ ($\gamma_{Sd\,(D=1)}$), and in the 19 realizations/samples studied in the text with sampling dimension $D_S = \log 19/\log 2^{12} = 0.35$; effective dimension $D+D_s = 1.35$ ($\gamma_{sd}\,(D=1.35)$). Since γ_D and $\gamma_{sd\,(D=1)}$ are very close, the hyperbolic behaviour of the tails is very hard to discern on a single river flow series.

all individual flow series and to the normalized flow series. The probability of exceedances as a function of quantile (s) for the normalized flow series is shown in Fig. 4c. It can be seen on a log–log plot that the distribution curves slowly; the logarithmic derivative at the extreme low probability end is an estimate of the best-fit asymptotic hyperbolic distribution, i.e., that closest to the multifractal model but with a different slope. The magnitudes of the slopes of the extreme tails obtained from the GEV distribution are given in Table 4 and are shown graphically in Fig. 5. Although the tail of the GEV fitted distribution shows similar behavior (i.e., on a log–log plot the distribution curves slowly), the magnitudes of the slopes are mostly higher than those of the q_D and q_s given by the multifractal model (Table 4). For the normalized flow series, the values of the exponents q_D and q_s were respectively obtained as 3.48 ± 0.64 and 3.12 ± 0.70, whereas the slope of the tails for the GEV is 4.5; this implies that the GEV distribution always underestimates the extremes. Note that the observed scaling of the flow statistics as a function of the aggregation scale x implies that the annual flood series are

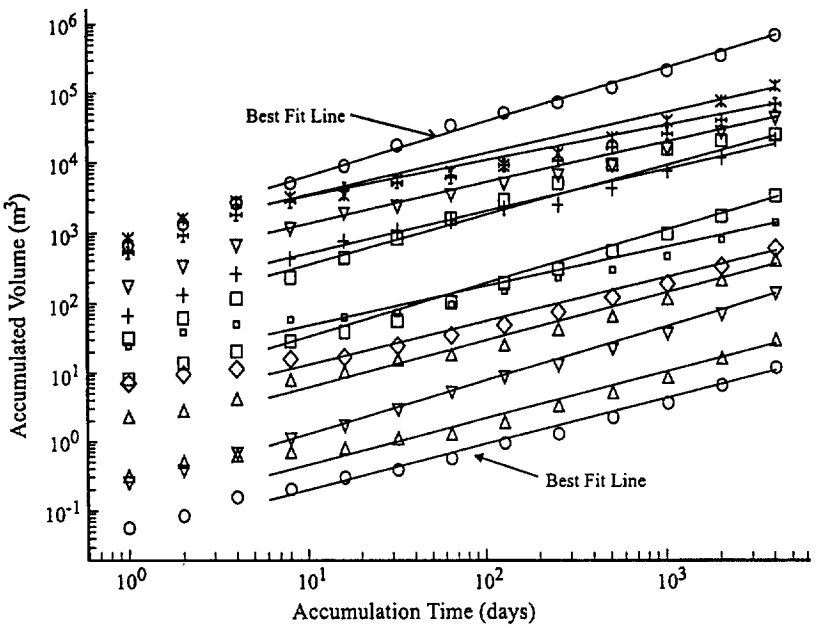

Fig. 7. Accumulated runoff volume for different time periods. The best fit is the slope (= 1 − γ max) of the fitted line using the accumulated volume from 8 days to 4096 days (from top to bottom: Mississippi River, Susquehanna River, Arkansas River, Osage River, Colorado River, Sabine River, Grand River, Ohoopee River, McCloud River, Rio Grande River, Canadian River, Indian Creek, Pecos River, Yantic River, North Nashua River, Kettle Brook, Mill River, Pendleton Hill River and Rocky Brook).

not independent of each other. This violates the basic assumption of fitting the GEV and the Gumbel distribution to the observed daily river flow data (see also Bendjondi, H. et al. 1997).

6. The scaling of extreme flow volumes

Estimates of maximum flow volumes at a variety of aggregation scales are needed in various water resource management problems such as storage planning, flood control, in the estimation of the maximum yield, etc. Hubert et al. (1993) gave a simple multifractal theory to estimate the maximum accumulated rainfall volumes is the maximum order of singularity for ϕ. Using Eq. (2), the maximum accumulated volume in time τ scale of resolution $\lambda = T/\tau$, is given as

$$(\mathrm{Vol})_\tau = \tau Q\tau \propto \tau^{1-\gamma} \tag{18}$$

Thus multifractal theory shows that the slope of the plot between the maximum volume and τ should be algebraic. In order to characterize the maximum accumulated volume, we need only estimate γ_{max}, where γ_{max} is the maximum order of singularity of the flow rate. Although models exist with a finite upper bound on γ (e.g. microcanonical cascades, the α-model, the log Poisson model, or universal multifractal with $\alpha < 1$), in general, the process will be unbounded (in particular, as here when $\alpha \geq 1$) and the actual sample maximum will depend on the sample size (shown in Fig. 6) and be equal to the sampling singularity γ_s, introduced earlier. For a single realization the dimension of the set of extreme events on the time axis must >0, hence $c(\gamma) = 1$. Hence, using Eq. (4), for a conservative multifractal process Hubert et al. (1993) obtained:

$$\gamma_s = \alpha' C_1^{1/\alpha} - \frac{C_1}{\alpha - 1} \tag{19}$$

in which α' is the exponent such that $1/\alpha + 1/\alpha' \leq 1$ and γ_s. The effective order of singularity (γ_s) estimated above is the singularity for the underlying conserved process. Since river runoff (Q) is obtained from the conserved process (ϕ) by a fractional integration of order H, for high enough order singularities this is equivalent to a shift in the order of singularities ($(Q_\tau d\phi_\tau \tau^H)$ i.e., $\gamma \rightarrow \gamma - H$); hence we obtain $Q_\tau \approx \tau^{-\gamma_{max}}$ with $\gamma_{max} = \gamma_s - H$. Since $H \approx 0$ for rainfall at these scales, Hubert et al. (1993) did not explicitly take this effect into account.

The plots of the observed maximum accumulation volume as a function of the time scale (τ) are shown in Fig. 7; the slopes = $1 - \gamma_{max}$. The straight lines are the regression estimates using the aggregated volumes at 8 days and larger time scales (i.e., low frequency regime). The estimated values of the relevant exponents for all individual stations are given in Table 4. Based upon the analysis, two inferences were made. First, as predicted, there exists a linear log–log (scaling) relationship between the observed maximum and the accumulated time (Fig. 7). Second, the estimated $(1 - \gamma_{max})$/slopes from different rivers yield estimates of γ_{max} which are close to the theoretical value $\gamma_s - H$ (Table 4). For some stations, there is a break in the scaling at around one week. This observation is compatible with that from spectral analysis, which also showed a break in the scaling regime at around the same period. The theoretical values of γ_s (or γ_{sd} whenever $q_D < q_s$) estimated from the multifractal parameters (C_1 and α) are given in Table 4. The average theoretical value of $\gamma_{max} = \gamma_s - H$ is 0.33 ± 0.2 and that obtained from the scaling of the extremes is 0.39 ± 0.13 (note that, in any case, γ_s and γ_{max} are both expected to have some random series to series variability since γ is a random variable). The closeness of γ_{max} and $\gamma_s - H$ shows that the scaling of the accumulated maximum volumes may well be the direct consequences of the multifractal nature of the river flows and are correctly estimated from the multifractal parameters. This implies that the multifractal model can indeed be used to satisfactorily model the maxima of the river flow series over a wide range of time scales (including presumably even extrapolating to longer scales than the length of the records since the scaling in Fig. 7 appears to continue to the largest observed scales).

7. Conclusions

Multifractal analysis of the daily river flow data from 19 river basins of varying watershed areas was carried out. The initial analysis of the scaling nature and its limits were assessed using spectral analysis.

For most of the rivers, there is a break in the scaling regime at a period of about one week. This time is roughly half of the atmospheric synoptic maximum, which is the typical lifetime of planetary-scale atmospheric structures including rain events. In general, for the river flows studied here, no upper limit for scaling regimes was found (for some river basin the series is more than 73 years long). The magnitude of spectral slope for the low frequency region varied from 0.73 to 1.88 with an average value of 0.72 for the normalized ensemble. It was also observed that the variability in the spectral slope and scaling is almost independent of the area of the basin considered, even though the latter varies over nearly 6 orders of magnitude.

For all individual flow series, as well as for the normalized flow ensemble of the universal multifractal parameters characterizing the infinite hierarchy of scaling exponents were estimated. Those parameters were in close agreement with those reported by Tessier et al. (1996) on much smaller basins. The variations of the multifractal parameters with the basin area suggests that the basin-to-basin variability was random rather than systematic. Using the observed flow series, the critical exponents (q_D) characterizing the multifractal phase transition and self-organized criticality (i.e., algebraic decay of the extremes) were estimated. On the basis of the present findings, the maximum order of moments that can be safely estimated using the daily river data lies (depending on the river) between 2 and 5. All the higher moments will be dominated by a single extreme value in the series. The algebraic fall-off of the extremes was most clearly observed in the ensemble distribution of normalized flows. The values of α also show that the order of singularities is in general not bounded. This algebraic decay of the probability distribution also brings into question the routine fitting of probability distributions with exponential tails (e.g., by using GEV statistics). It was also observed that the universal multifractal parameters were able to describe the scaling behavior of the maximum accumulations from nearly one week to the limit of the series (more than 11 years).

The work here provides the basis for using universal multifractal models for various engineering problems, including the (causal) transfer functions for modelling the rainfall runoff process including the flow generating processes (e.g. precipitation) and the factors that modify the flow of water through the basin (e.g. topography). Another potential application of multifractal flow models is to disaggregate the statistical properties of the river flow series from larger time scales (say year) to shorter resolution (say month or week). Most of all, the multifractal model, which is based upon the physical symmetry principle of scale invariance, could provide a sound theoretical basis for the entire flood frequency procedure, which so far has been quite ad hoc.

References

Bak, P., Tang, C., Weissenfield, K., 1987. Self-organized criticality: an explanation of $1/f$ noise, Phys. Rev. Lett., 59, 381–384.

Bak, P., Tang, C., Weissenfield, K., 1988. Self-organized criticality, Phys. Rev. A, Gen. Phys., 38, 364–374.

Bak, P., Chen, K., Tang, C., 1990. A forest-fire model and some thoughts on turbulence, Phys. Lett. A, 147, 297–300.

Bendjondi, H., Hubert, P., Schertzer, D., Lovejoy, S., 1997. Multifractal point of view on rainfall-intensity-duration-frequency curves. Comptes Readus Acad des Sci, 325, pp. 323–326.

Benson, M.A., 1962. Factors influencing the occurrence of floods in a humid region of diverse terrain. US Geological Survey, Water Supply Paper 1580-B, 63 pp.

Benson, M.A., 1964. Factors affecting the occurrence of floods in the south west. US Geological Survey, Water Supply Paper 1580-D, 69 pp.

Brax, P., Peschanski, R., 1991. Levy stable law description of intermittent behaviour and quark gluon plasma phase transitions, Phys. Lett. B, 253 (1-2), 225–230.

Cunnane, C., 1988. Methods and merits of regional flood frequency analysis, J. Hydrol., 100, 269–290.

Davis, A., Marsak, A., Wiscombe, A., Cahalan, R., 1994. Multifractal characterization of nonstationary and intermittency in geophysics; observed, retained or simulated, J. Geophys. Res., 99, 8055–8072.

Dooge, J.C.L., 1986. Looking for hydrologic laws, Water Resour. Res., 22 (9), 465–585.

Duncan, M., 1993. The universal multifractal nature of radar echo fluctuations. PhD thesis, McGill University.

Evertsz, C.J.G. and Mandelbrot, B.B., 1992. Multifractal measures. In: Peitgen, H.O., Jurgens, H. and Saupe, D. (Eds.), Chaos and Fractals. Springer-Verlag, New York, pp. 921–953.

Fraederich, K., Larnder, C., 1993. Scaling regimes of composite rainfall time series, Tellus, A45, 289–298.

Gabriel, P., Lovejoy, S., Schertzer, D., Austin, G.L., 1988. Multifractal analysis of resolution dependence in satellite imagery, J. Geophys. Res., 15, 1373–1376.

Gupta, V.K., Waymire, E., 1993. A statistical analysis of mesoscale rainfall as a random cascade, J. Appl. Meteorol., 32, 251–267.

Gupta, V.K. and Waymire, E., 1997. Spatial variability and scale

invariance in hydrologic regionalization. In: Spostio, G. (Ed.), Scale Invariance and Scale Depedence in Hydrology. Cambridge University Press (in press).

Gupta, V.K., Messa, O.J., Dawdy, D.R., 1994. Multi scaling theory of flood peaks: regional quantile analysis, Water Resour. Res., 30 (12), 3405–3421.

Haktanir, T., 1992. Comparison of various flood frequency distributions using annual flood peaks data of river Anatolia, J. Hydrol., 136, 1–31.

Hosking, J.R.M., Wallis, J.R., Wood, E.F., 1985. An appraisal of the regional flood frequency procedure in the UK flood studies report, Hydrol. Sci. J., 30 (1), 85–109.

Hubert, P., Tessier, Y., Lovejoy, S., Schertzer, D., Schmitt, F., Ladoy, P., Carbonnel, J.P., Violette, S., Desurosne, I., 1993. Multifractals and extreme rainfall events, Geophys. Res. Lett., 20 (10), 931–934.

Hurst, H.E., 1951. Long-term storage capacity of reservoirs, Trans. Am. Soc. Civ. Eng., 116, 770–808.

Ijjasz-Vasquez, E.J., Rodriguez-Iturbe, I., Bras, R.L., 1992. On the multifractal characterization of river basins, Geomorphology, 5 (3-5), 297–310.

Klemes, V., 1986. Dilettantism in hydrology: transition of destiny, Water Resour. Res., 22 (9), 1775–1885.

Koloshnikova, V.N., Monin, A.S., 1965. Spectra of meteorological field fluctuations, Izvestiya Atmos. Ocean. Phys., 1, 653–669.

Lavallee, D., Lovejoy, S. and Schertzer, D., 1993. Nonlinear variability and landscape topography: analysis and simulation. In: DeCola, L. and Lam, N. (Eds.), Fractals in Geography. PTR Prentice-Hall, pp. 158–192.

Lettenmaier, D.P., Potter, K.W., 1985. Testing the flood frequency estimation models using a regional flood generation model, Water Resour. Res., 21 (12), 1903–1913.

Liu, H.H., Molz, F.J., 1997. Multifractal analysis of hydraulic conductivity distributions, Water Resour. Res., 33 (11), 2483–2488.

Lovejoy, S., 1981. Analysis of rain areas in terms of fractals, 20th Conf on radar meteorology, pp. 476–84, AMS, Boston.

Lovejoy, S., 1982. The area-perimeter relations for rain and cloud areas. Science, 216, 185–7.

Lovejoy S., Mandelbrot, B., 1985. Fractal properties of rain and a fractal model. Tellus, 37A, 209–32.

Lovejoy, S., Schertzer, D., 1986. Scale invariance in climatological temperatures and the spectral plateau, Ann. Geophys., 4B, 401–410.

Lovejoy, S., Schertzer, D., 1990. Fractals, rain drops and resolution dependence of rain measurements, J. Appl. Meteorol., 29, 1167–1170.

Lovejoy, S., Schertzer, D., 1990. Multifractals, universality classes and satellite and radar measurements of cloud and rain fields, J. Geophys. Res., 95, 2021–2034.

Lovejoy, S. and Schertzer, D., 1995. Multifractals and rain. In: Kunzewicz, Z.W. (Ed.), New Uncertainty Concepts in Hydrology and Water Resources. Cambridge University Press, pp. 61–103.

Lovejoy, S., Schertzer, D., Tsonis, A.A., 1987. Functional box counting and the multiple dimensions in rain, Science, 235, 1036–1038.

Lovejoy, S., Schertzer, D., Silas, P., Tessier, Y., Lavallee, D., 1993. The unified scaling model of atmospheric dynamics and systematic analysis of scale invariance in cloud radiation, Ann. Geophys., 11, 119–127.

Lovejoy, S., Lavallee, D., Schertzer, D., Ladoy, P., 1995. The $L^{1/2}$ law and multifractal topography: theory and analysis, Nonlin. Process. Geophys., 2 (1), 16–22.

Lovejoy, S., Duncan, M., Schertzer, D., 1996. The scalar multifractal radar observer's problem and rain, J. Geophys. Res., 101 (D21), 26479–26492.

Lovejoy, S., Schertzer, D. and Silas, P., 1998. Diffusive transport in 1-D multifractal porous media. Water Resour. Res. (submitted).

Mandelbrot, B.B., Wallis, J.R., 1968. Noah, Joseph and operational hydrology, Water Resour. Res., 4, 909–918.

Mandelbrot, B.B., Wallis, J.R., 1969. Some long run properties of geophysical records, Water Resour. Res., 5, 228.

Marsan, D., Schertzer, D., Lovejoy, S., 1996. Causal space–time multifractal processes: predictability and forecasting of rain fields, J. Geophys. Res., 101 (D21), 26333–26346.

Natural Environmental Research Council, 1975. Flood Studies Report, Vol. 1. London.

Oldham, K.B. and Spanier, J., 1974. The Fractional Calculus. Academic Press, New York.

Olsson, J., Niemczynowicz, J., Brendtsson, R., 1995. Limits and characteristics of the multifractal behavior of a high resolution rainfall time series, Nonlin. Process. Geophys., 2 (1), 23–29.

Olsson, J., Niemczynowicz, J., Brendtsson, R., 1995. Fractal analysis of high resolution rainfall time series, J. Geophys. Res., 98 (12), 23265–23274.

Over, T.M., Gupta, V.K., 1996. A space-time theory of mesoscale rainfall using random cascades. J. Geophys Res, 101, 26319–31.

Parisi, G., Frisch, U., 1985. A multifractal model of intermittency, turbulence and predictability in geophysical fluid dynamics and climate dynamics, 87–88, Ghil, Benzi, Paris, (eds), North-Holland.

Pilgrim, D., 1986. Bridging the gap between flood research and design practice, Water Resour. Res., 22 (9), 1655–1765.

Potter, K.W., Lettenmaier, D.P., 1990. A comparison of flood frequency estimation methods using a resampling method, Water Resour. Res., 26 (3), 415–424.

Rinaldo, A., Rodriguez-Iturbe, I., Rigon, R., Bras, R.L., Ijjasz-Vasquez, E., Marini, A., 1992. Minimum energy and fractal structure of drainage net works, Water Resour. Res., 28 (9), 2183–2195.

Rodriguez-Iturbe, I., Rinaldo, A., Rigon, R., Bras, R.L., Marini, A., Ijjasz-Vasquez, E., 1992. Energy dissipitation, runoff prediction and the three dimensional structure of river, Water Resour. Res., 28 (4), 1095–1103.

Ross, B., 1975. Fractional calculus and its applications. Lecture Notes in Mathematics, Vol. 475. Springer, New York, 381 pp.

Salas, J.C., 1993. Analysis and modeling of hydrologic time series. In: Maidment, D.R. (Ed.), Handbook of Hydrology. McGraw-Hill, New York, pp. 19.1–19.72.

Schertzer, D. and Lovejoy, S., 1985. Generalized scale invariance, in turbulent phenomena, Physico-Chem Hydrodyn J, 6, 623–35.

Schertzer, D., Lovejoy, S., 1987a. Singularités ansotrope, divergence des moments en turbulence, Ann. Soc. Math. Québec, 11 (1), 139–181.

Schertzer, D., Lovejoy, S., 1987b. Physical modeling and analysis of rain and clouds by anisotropic scaling of multiplicative processes, J. Geophys. Res., D8 (8), 9693–9714.

Schertzer, D. and Lovejoy, S., 1989. Nonlinear variability in geophysics: multifractal analysis and simulations. In: Pretronero, L. (Ed.), Fractals: their Properties and Origins. Plenum Press, New York, pp. 49–79.

Schertzer, D., Lovejoy, S., 1997. Universal multifractals do exist!, J. Appl. Meteorol., 36, 1296–1303.

Schertzer, D. and Lovejoy, S., 1998. The multifractal phase transition route to self-organized criticality. Phys. Rep. (in press).

Schertzer, D., Lovejoy, S., Lavallee, D. and Schmitt, F., 1993. Generic multifractal phase transitions and self-organized criticality. In: Pendlang, J.M. and Lejeune, A. (Eds.), Cellular Automata: Prospects in Astrophysical Applications. World Scientific, pp. 216–227.

Schertzer, D., Lovejoy, S. and Schmitt, E., 1995. Structures in turbulence and multifractal universality. In: Meneguzzi, M., Pouquet, A. and Salem, P.L. (Eds.), Small Scale Structures in 3D and MHD Turbulence, Springer-Verlag, Berlin. Lecture notes in Physics, 462, 137–144.

Schertzer, D., Lovejoy, S., Schmitt, F., Chigirinskaya, Y., Marsan, D., 1997. Multifractal cascade dynamics and turbulent intermittency, Fractals, 5, 427–521.

Strahler, A.N., 1964. Quantitative geomorphology of drainage basins and channel networks. In: Chow, V.T. (Ed.), Handbook of Applied Hydrology, Sect. 4. McGraw-Hill, New York, pp. 39–76.

Tessier, Y., Lovejoy, S., Schertzer, D., 1993. Universal multifractals: theory and observations for rain and clouds, J. Appl. Meteorol., 32 (2), 223–250.

Tessier, Y., Lovejoy, S., Hubert, P., Schertzer, D., Pecknold, S., 1996. Multifractal analysis and modeling of rainfall and river flows and scaling, causal transfer functions, J. Geophys. Res., 101 (D21), 26427–26440.

Thomas, D.M. and Benson, M.A., 1970. Generalization of streamflow characteristics from drainage basin characteristics. US Geological Survey, Water Supply Paper 1975, 75 pp.

Turcotte, D.L., Greene, A., 1993. A scale invariant approach to flood-frequency analysis, Stoc. Hydrol. Hydraul., 7, 33–40.